heritage

Article

The Long-Term Efficiency and Compatibility of Hydrophobic Treatments in Protecting Vulnerable Sandstone at Arbroath Abbey (Scotland)

Marli de Jongh [1,*], David Benavente [2], Maureen Young [3], Callum Graham [3] and Martin Lee [4]

[1] British Geological Survey (BGS), Nicker Hill, Keyworth, Nottingham NG12 5GG, UK
[2] Departamento de Ciencias de la Tierra y del Medio Ambiente, Universidad de Alicante, Alicante 03690, Spain; david.benavente@ua.es
[3] Historic Environment Scotland (HES), The Engine Shed, Forthside Way, Stirling FK8 1QZ, UK; maureen.young@hes.scot (M.Y.); callum.graham@hes.scot (C.G.)
[4] School of Geographical and Earth Sciences, University of Glasgow, University Avenue, Glasgow G12 8QQ, UK; martin.lee@glasgow.ac.uk
* Correspondence: marli@bgs.ac.uk

Abstract: The application of hydrophobic treatments as a means of protecting vulnerable stone heritage has been a topic of research for decades. The findings of previous research have shown that there are a number of factors that influence the efficiency of a treatment and that sometimes, if used incorrectly, such treatments can even accelerate stone weathering and decay. In this study, we revisit a hydrophobic treatment test area at Arbroath Abbey where the product was applied over 40 years ago, thus providing a rare opportunity to investigate the long-term efficiency of hydrophobic treatments. As well as assessing the condition of the treated area in situ by means of moisture analyses, lab-based accelerated salt weathering experiments are conducted to better understand the impact of silane-based treatments on sandstone durability. Moreover, the petrography and petrophysical properties of weathered sandstone (open porosity, capillary absorption, and vapour diffusion) before and after treatment are also characterised to provide a better understanding of how stone properties may influence the compatibility of the treatment. The field-based results show that the treated area has maintained a degree of hydrophobicity since its application over 40 years ago. Both field-based and lab-based analyses suggest that silane-based treatments can be used successfully in protecting sandstone when applied correctly, both in reducing the rate of decay and functioning over long periods of time. However, sandstone heterogeneity may mean that some individual stones are less compatible with the hydrophobic treatment tested than others. Further field-based analyses (including methods such as XRF and in situ vp) of the treated area is required in order to determine the state of conservation more accurately. These results highlight the complexity in selecting a suitable hydrophobic treatment, especially at built sites where the mineralogy and petrophysical properties of the stone may vary between blocks. However, such treatments may still be important to consider as many climates, including Scotland's, are becoming progressively wetter, increasing the vulnerability of stone heritage to moisture ingress, accelerated decay, and eventual ruin.

Keywords: sandstone; decay; heritage; hydrophobic; conservation; buildings; treatments; petrology

Citation: de Jongh, M.; Benavente, D.; Young, M.; Graham, C.; Lee, M. The Long-Term Efficiency and Compatibility of Hydrophobic Treatments in Protecting Vulnerable Sandstone at Arbroath Abbey (Scotland). *Heritage* **2023**, *6*, 4864–4885. https://doi.org/10.3390/heritage6070259

Academic Editors: Nick Schiavon, Mauro Francesco La Russa and Patricia Sanmartín

Received: 11 May 2023
Revised: 9 June 2023
Accepted: 16 June 2023
Published: 21 June 2023

1. Introduction

This study is an investigation into the use of hydrophobic treatments as a means of protecting sandstone by reducing the rate of stone decay and uses as a case study Arbroath Abbey (Figure 1A,B). Situated on the east coast of Scotland, the Abbey was founded in 1178 and constructed using local sandstone from the nearby coast. It has undergone frequent episodes of restoration, and the original Abbey stone has been replaced extensively.

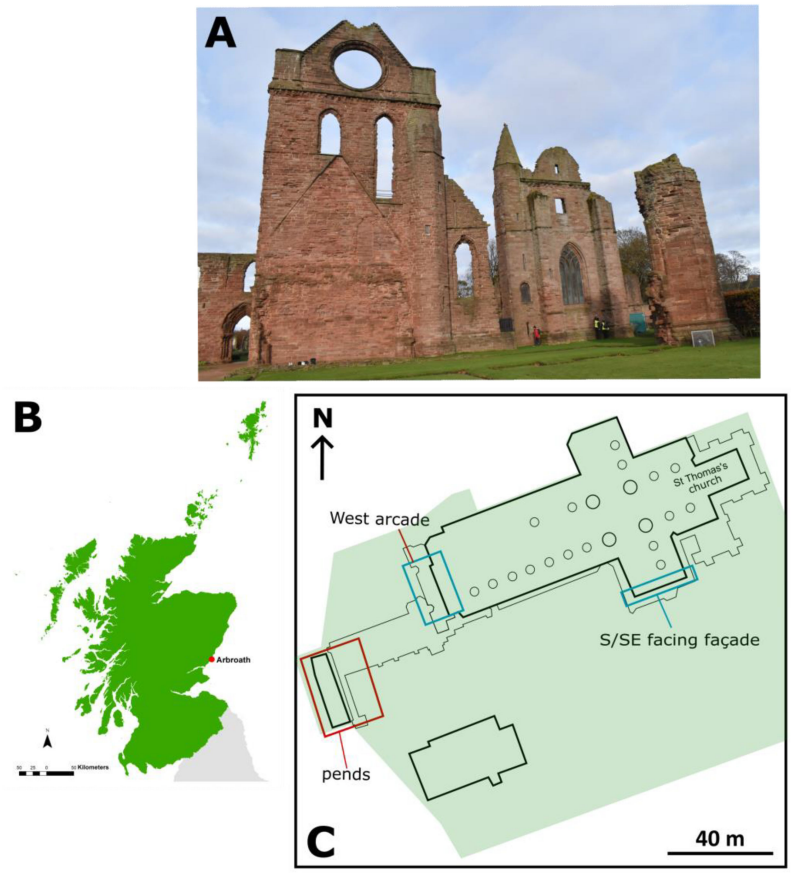

Figure 1. (**A**,**B**) Arbroath Abbey (shown in image) located on the East Coast of Scotland; (**C**) basic layout of the ruinous Abbey. The red box denotes the pends area from where samples were taken. The blue boxes are areas that had hydrophobic treatments in 1976. The base of two columns in the west arcade, and a relatively small area of a façade were treated. The S/SE facing façade is where moisture analysis was conducted. Green area denotes area of the Abbey including the grounds. Figure contains Ordnance Survey data © Crown copyright and database right 2023.

In 1976, a silane-based treatment, Brethane, was applied (by brush) to several areas of Arbroath Abbey: the base of two columns located in the west arcade and a S/SE facing façade (Figure 1C) [1]. Brethane is a hydrophobic silane-based treatment and was developed by the Building Research Establishment before being trialed at different sites around the UK between 1976 and 1979 [2]. Brethane was a mixture of methyltriethoxysilane, methylated spirit mixed with water and a solution of lead octoate (Pb-36) in white spirit. It never became commercially available, however, due to health and safety concerns regarding the presence of lead [3]. As well as monitoring the performance of Brethane at different sites, lab-based experiments were also conducted to assess the efficiency of Brethane in protecting limestones and sandstones [4]. Despite promising results showing that the application of Brethane reduced rates of stone decay, the lack of information regarding the long-term behaviour of Brethane and silane-based products in general limited the understanding of the efficiency of hydrophobic treatments in protecting stone-built heritage. At Arbroath Abbey, there have been two formal inspections since the brethane application, both of which describe the treated stone as appearing sound with no visually discernible changes or obvious detrimental impact to its integrity [1].

Protective treatments for sandstone more broadly have been studied extensively [5–11]. The two primary subdivisions of treatment are protective coatings and consolidants [12]. Coatings are typically hydrophobic and aim to prevent an ingress of liquid water (rain, saline solutions, etc.) and, therefore, reduce weathering and subsequent decay. Consolidants, on the other hand, aim to strengthen stone by increasing cohesion by cementing

the constituent grains together [12], and they can also have a hydrophobic element [1]. Researchers have noted several specific concerns with regards to the compatibility of protective treatments with porous sandstones. The application of treatments can lead to the modification of physical stone properties, such as changes in vapour diffusion properties, hygric/hydric dilatation, and the mechanical strength of the surface [13,14]. Changes in pore structure properties may affect how moisture and salts move through the stone, the latter being important in the case of Arbroath given its coastal location. Previous research has found that in some instances, crystallised salts can accumulate and become trapped behind the hydrophobic surface layer, accelerating physical weathering through decay patterns, such as spalling [15–17]. Many studies that evaluate the potential use of hydrophobic treatments in protecting stone rely mostly on data obtained from lab-based accelerated weathering experiments. Despite the useful data obtained using such methods, they fail to accurately replicate natural conditions, as it can be difficult to recreate the decadal timescales of natural weathering within a three–four week long experiment. Therefore, lab-based experiments are most useful when considered together with in situ field analyses that assess the long-term behaviour of such treatments in a natural environment.

The aim of the study was to understand the potential use of silane-based treatments in the protection and conservation of weathered sandstone at Arbroath Abbey through both in situ and lab-based investigations. First, we conduct moisture mapping of an area at Arbroath Abbey, previously treated with a silane-based hydrophobic product, for the first time since the application over 40 years ago. Second, we assess the compatibility of a currently available silane-based hydrophobic product with weathered sandstone from the Abbey through salt weathering experiments and characterisation of stone properties. Both Brethane and the treatment selected for lab-based experiments are silane-based hydrophobic products. In situ moisture analyses offers insight into the long-term efficiency of silane-based treatments, revealing whether the hydrophobic layer is still preventing the intrusion of liquid water into the stone. Salt weathering experiments offer insight into the compatibility of such treatments by showing the relative difference in decay between untreated and treated sandstone samples. Moreover, the petrography and petrophysical properties of weathered sandstone (open porosity, capillary absorption, and vapour diffusion) before and after treatment are also characterised to provide a better understanding of how stone properties may influence the compatibility of the treatment. This study used two weathered blocks, a lintel and corbel, obtained from Historic Environment Scotland during restoration work at the Abbey in 2019. The mineralogy and petrography of both blocks was studied in detail not only to assess the compatibility of the hydrophobic treatment, but also to understand mineralogical and textural variations in the stone. Sampling at sites of high heritage value is often heavily restricted, and sampling is limited to the outer weathered crust of masonry units. Unfortunately, a lack of sampling commonly hinders scientific progress in the field of heritage science and limits our understanding of best conservation practices at a given site [18]. Obtaining two blocks from a built site of such cultural value is very unusual and offers a rare opportunity to fully characterise and experiment on the historic stone.

2. Materials

2.1. Samples of Abbey Stone

Two weathered sandstones from Arbroath Abbey were used in this study and consisted of a large lintel block, designated A-L, and large corbel block, designated A-C (~50 cm × 20 cm × 20 cm). The blocks were removed from the Abbey during 2019 restoration work and are thought to have been part of the original construction, which began in 1178. Based on the age of the Abbey and the petrological and physical properties of sandstone, this sandstone was likely sourced from the nearby coast, which geologically formed part of the Scone Sandstone Formation (deposited during Devonian times in a semi-arid climate and fluvial environment). Upon initial inspection, the blocks differed slightly in colour and mineralogy. The A-C sandstone had a deep red-brown colour while A-L

was comparatively lighter with a cream-pink colour (Figure 2). There was strong mineral alignment of mica in A-L while A-C exhibited planar bedding on a scale of ~1 mm.

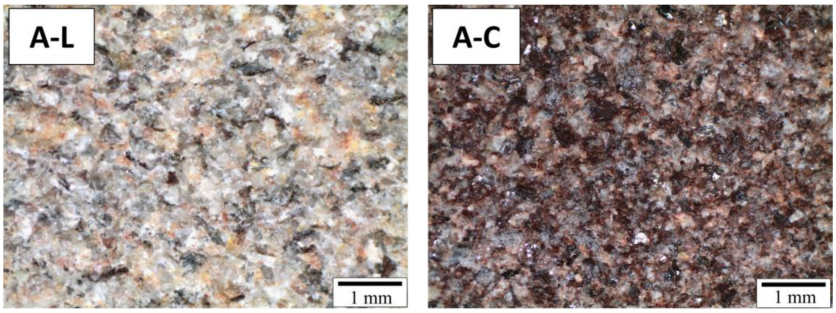

Figure 2. Binocular microscope images of sandstones A-L and A-C. Both sandstones are thought to date back to original construction, which started in 1178.

2.2. Hydrophobic Treatment

The commercial water repellent Brethane could not be used in the present study as it is no longer manufactured. Instead, a hydrophobic cream was used and was selected based on several factors. First, the capillary absorption coefficient (w-value) of the original sandstone was used to identify a recommended penetration depth of the water repellent of 7 mm (minimum) [19,20]. Based on the minimum desired penetration depth, open porosity, and estimated application time, a hydrophobic cream was chosen [20]. The choice of cream over a liquid agent was primarily due to the relatively low capillary absorption rates of sandstone samples, thus requiring a longer application time for sufficient penetration of treatment. Cream took longer to completely dry, allowing the treatment to penetrate the sample to a sufficient depth before fully curing. Table 1 summarises some of the properties of the cream, including its composition and curing time.

Table 1. Characteristics of selected commercial hydrophobic masonry cream.

Hydrophobic Cream Property	Description
Composition	Silane/siloxane masonry cream containing: hydrocarbons (C_{11}–C_{14}); isoalkanes; cyclics; <2% aromatics; and triethoxyoctylsilane
Density	0.86 g/cm^3
Coverage	5 m^2 per litre (single coat recommended)
Curing time (time between application and post-application experiments)	28 days

3. Methods

3.1. Field Observations

The treated test area was first located during an initial visit in 2017. This was determined by pipetting water across the entire façade to locate the boundary of the treated area by monitoring how the pipetted liquid water interacted with the stone substrate. In addition to this preliminary test, decay patterns at the Abbey were described according to the ICOMOS-ISCS (2008) illustrated stone glossary [21]. According to the glossary, decay patterns can be divided into five main categories: cracks and deformation, detachment, features induced by material loss, discolouration and deposit, and biological colonisation.

3.2. Moisture Analysis

A microwave moisture meter was used to evaluate the relative differences in moisture content on the façade (~7.5 m length) that was partially treated with Brethane in 1976 (Figure 3). This analysis was carried out in July 2019 after several consecutive days of dry

weather. Two measurements were obtained per block, creating an eighteen-point vertical transect, where each transect was 15 cm apart and total number of points analysed was 918. Three different probe heads, which detect water at varying depths (15 cm, 30 cm, and 80 cm), were used, and the stone façade was mapped prior to wetting. After this initial mapping, a smaller region containing the treated façade and adjacent untreated area was wetted using a pressurised hose system before being mapped again. The data were analysed using MoistTools software, which interpolates data between measured data points.

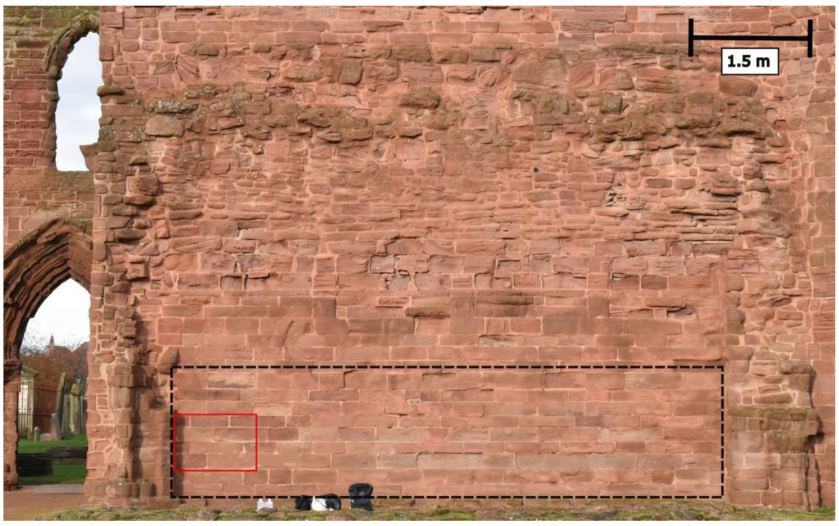

Figure 3. Image of the studied façade at Arbroath Abbey. Black box outlines the boundaries of the area analysed by the moisture meter, and the red box outlines the boundaries of the area that previously had a hydrophobic treatment.

3.3. Application of Hydrophobic Cream

The cream was applied to cubic samples (length 50 mm) of A-C and A-L, which were first dried to a constant mass using an oven at 105 °C. Any loose debris was gently removed from the surface using a small brush. A single coat of cream was applied using a small paint roller as recommended by the product's manufacturer. Alternatively, the treatment can be applied using a brush or spray. Once the treatment had been applied, the samples were left to cure at conditions of 20 ± 1 °C and 50 ± 5 RH for at least 28 days prior to any post-application experiments. The number of faces of each sample coated with the cream depended on the analysis to be carried out. Samples for capillary absorption experiments and salt weathering were coated on every face while samples for vapour diffusion analysis were coated on one face only.

3.4. Mineralogy and Petrography

The mineralogical composition of the sandstones was determined using powdered X-ray Diffraction (XRD), and analyses were carried out using a Thermo Electron ARL X'TRA XRD. The settings were as follows: CuKα radiation, running at 45 mA and 44 kV, step size of 0.02°, and a scan rate of 1° per minute. Mineral peaks were identified using the 2018 International Centre for Diffraction Data (ICDD) database and Sieve software (part of the ICDD database package). Mineralogy of both the bulk sandstone and clay fraction were analysed. Clay minerals were extracted by mixing the crushed bulk sample with deionised water in a centrifuge tube before placing in an ultrasonic bath. The sample was then placed in a centrifuge chamber under conditions that left only the 2 µm grain size fraction in suspension. The water containing the suspended clay minerals was then carefully pipetted into a glass jar and left on a hot plate to dry at ~50 °C. The dried clay was then removed from the jar and gently mixed in a mortar and pestle before being mounted on to a glass slide using the filter suction method to align clays. The extracted clay fractions

characterised were from: the weathered surface of both A-L and A-C and the interior stone of both A-C and A-L. Salts were also extracted from both weathered stones and analysed using XRD using a similar extraction method for that of clay minerals.

Petrographic characterisation was carried out using an FEI Quanta 200 F Environmental Scanning Electron Microscope (SEM). The SEM was used to evaluate sandstone mineralogy and texture, including the distribution of clay minerals. Polished thin sections were sputter coated with carbon for analysis. The SEM was operated at high vacuum, at 20 kV, using backscattered (BSE) and secondary electron (SE) imaging, and qualitative EDX. In addition to thin section analysis, small gold-coated chips of stone were also analysed under the same conditions.

3.5. Open Porosity and Bulk Density

Open porosity and apparent dry bulk density were determined by the vacuum saturation method according to BS EN 1936:2006 [22]. Cut sandstone samples were placed in a desiccator before the pressure inside the desiccator was reduced to 2 ± 0.7 kPa. Deionised water was then slowly introduced into the desiccator while maintaining the aforementioned pressure. Finally, once the samples were immersed in water, the desiccator pressure was gradually brought back to atmospheric pressure. The samples were left immersed overnight before a saturated weight, m_s, was taken the following day. The open porosity was then calculated and expressed as a percentage by comparing the saturated weight, dry weight, and volume of the sample using the following equation:

$$P_o = \frac{m_s - m_d}{v} \times 100 \quad (1)$$

where P_o = open porosity (%), v = volume of the sample (cm^3), m_s = saturated weight (g), and m_d = dry weight (g).

3.6. Water Vapour Diffusion Resistance

The water vapour diffusion experiment was carried out according to the BS EN 12572:2016 standard [23]. As previously discussed in the Introduction, the diffusion of water vapour through stone was essential to allow the free movement of water (and salts) and allow stone to dry thoroughly. The wet-cup test was used, and the set up for the experiments is shown in Figure 4A. For the test, samples were secured onto containers that held either distilled water or saturated solution (Figure 4B). The constructed sample was then placed into a controlled environment with specific RH and temperature (Figure 4). The difference in RH between the interior of the cup and the external chamber led to the diffusion of water vapour through a specified surface area, the rate of which was measured over time through changes in specimen mass.

Three samples of A-C and three samples of A-L were used. Sandstone dimensions for the experiment were 60 mm × 60 mm × 20 mm. After partly filling borosilicate glasses with distilled water, samples were secured onto glasses using tape and melted wax (60% microcrystalline wax and 40% paraffin wax). Care was taken to ensure the sample was sealed to the container properly. The mass of each constructed sample was then recorded before being placed into a desiccator, which was then put inside an incubator maintaining a temperature of 21 °C ± 1. The RH inside the cup was 100 while the RH outside the cup (desiccator) was maintained at 45 ± 5% using a saturated solution of potassium carbonate (K_2CO_3). Finally, as the maintained difference in RH between cup and desiccator was the driving force of the experiment, hygrochron ibuttons were placed inside the desiccator to continually monitor the temperature and RH throughout the experiment. The mass of the samples was recorded, and the ibuttons were checked every two days for four weeks. The wet-cup test was performed twice in this study, once prior to application of the treatment and once after application of the treatment using the same samples. The water vapour diffusion resistance factor, μ, was calculated through a series of expressions described in Table 2.

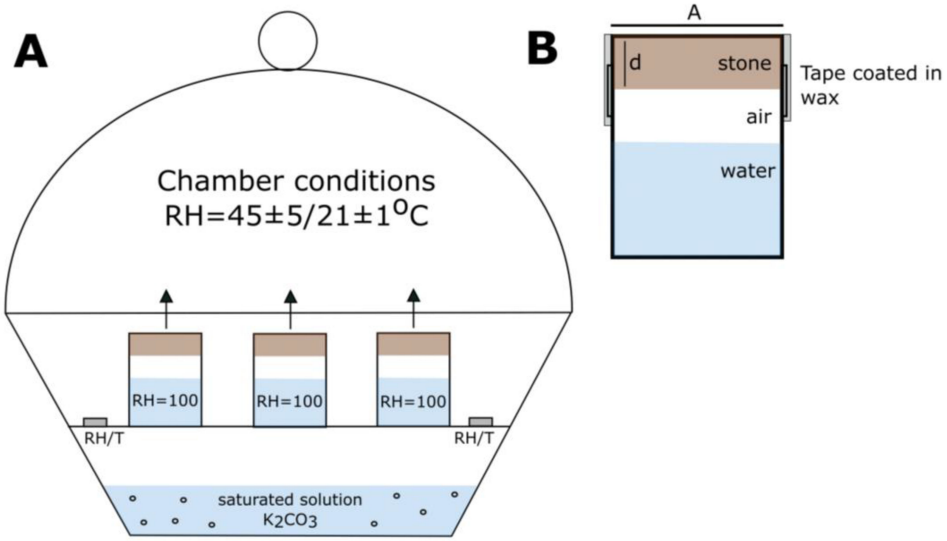

Figure 4. (**A**) Experimental set up and conditions used for the wet-cup test. Each desiccator contained three samples in total; (**B**) The sandstone samples, with measured thickness, d, were sealed to the cup using tape followed by melted wax. As well as securing the sample to the cup, the wax covers the exposed sides of the sandstone, therefore restricting the diffusion of vapour to the specified surface area, A.

Table 2. Summary of the series of equations used to determine the water vapour diffusion resistance factor, μ.

Equation Name	Equation	Values
Mass rate of change, Δm	$\Delta m = \frac{m_2 - m_1}{t_2 - t_1}$	Δm = change of mass per time for a single determination (kg/s); m_1 = mass of test assembly at time t_1 (s); m_2 = mass of test assembly at time t_2 (s). Water vapour flow rate, G, is then calculated as the mean of at least five successive determinations of Δm.
Vapour pressure difference, Δp	$\Delta p = RH \cdot 610.5 \cdot e^{\frac{17.269 \cdot T}{237.3 + T}}$	RH= relative humidity, and T = temperature (°C)
Water vapour permeance, W	$W = \frac{G}{A \times \Delta p}$	G = water vapour flow rate through the specimen (kg/s), A = area of specimen (m^2), and Δp = water vapour pressure difference.
Water vapour permeability, δ	$\delta = W \times d$	W = water vapour permeance [kg/(m^2·s·Pa)], and d = thickness of the sample (m).
Water vapour diffusion resistance factor, μ	$\mu = \frac{\delta air}{\delta}$	δair = water vapour permeability of air at 23 °C (for this experiment).

3.7. Capillary Absorption

Cubic sandstone samples (length 50 mm) were used to characterise the capillary absorption at two points: (a) before and after treatment with cream and (b) before and after the durability experiments. The samples were placed in a shallow tray of water and their mass was measured regularly over the course of a day according to BS EN ISO 15148:2002 [24]. The rate of capillary absorption was measured in two directions, parallel and perpendicular to the sedimentary bedding. During the experiment, the difference between the mass per weighing was calculated using the equation:

$$\Delta m_t = m_t - m_i \quad (2)$$

where Δm_t = change in mass (kg), m_t = mass value at the time of the weighing (kg), and m_i = initial mass value (kg).

Results were plotted as adsorbed water per unit area against the square root of time ($\sqrt{t}$). Capillary imbibition kinetics consisted of two stages: a first stage that defined water adsorption and a second stage defining saturation. The slope of the curve during water adsorption was the water absorption coefficient, C (kg/(m^2·h$^{0.5}$) and could be defined by the following equation:

$$C = \frac{m_t - m_i}{A \cdot \sqrt{t}} \quad (3)$$

where C = capillary water absorption coefficient (kg/(m^2·h$^{0.5}$), m_t = mass value at the time of the weighing (kg), m_i = initial mass value (kg), A = immersed bottom surface area (m^2), and $\sqrt{t}$ = time since the beginning of the experiment (h).

3.8. Ultrasonic Wave Velocities (V_p)

Compressive p-wave velocities (V_p) were measured on cubic samples using a Tektronix TDS 3012B 2 channel colour digital oscilloscope. An eco-gel visco-elastic couplant was used to allow for effective coupling of the transducer and each cubic sandstone sample. V_p was measured prior to, during, and at the end of the salt weathering experiment (described below) to aid in the determination of the extent of weathering of the untreated and treated samples.

3.9. Durability

The durability of the untreated and treated samples was determined via salt weathering experiments. The experiments used a non-standard method following Benavente et al. (2001) [25]. A non-standard method was selected as the experimental conditions were more realistic to how liquid water interacts with the stone substrate on site. The non-standard method, as used in this study, allowed capillary absorption of water through one face of the sample, whereas the standard method involves total immersion of the sample, which is less realistic to how liquid water interacts with a stone façade. The cubic samples (length 50 mm) were partially submerged in a Na_2SO_4 (conc. 14%) saline solution throughout the entire experiment, with the exception of a drying period that took place in an oven at 50 °C between cycles. The samples were placed in the solution so that capillary uptake was parallel to bedding, mimicking the direction that moisture penetrates the stone on site. The samples were subject to 20 temperature/RH cycles (10 °C/90% and 20 °C/50%) inside a climatic chamber. For each sandstone type, 12 samples were used where six were untreated and six were treated with the hydrophobic cream. To assess the extent of weathering, ultrasonic wave velocity (V_p, described above) was measured at the beginning of the experiment (prior to weathering), during the middle of the experiment (samples containing salts), and again at the end of the experiment (samples containing salts and salts extracted). Finally, the porosity and capillary absorption coefficient were measured before and after weathering to evaluate the effectiveness and durability of the treatment.

4. Results and Discussion

4.1. Decay Patterns at Arbroath Abbey

Upon initial inspection in 2017, the treated area of the S/SE facing façade still retains a degree of hydrophobicity, preventing water ingress some 40 years after the initial application of Brethane. This was determined by pipetting water across the entire façade to locate the boundary of the treated area and to determine whether or not the treated area was still hydrophobic. It was noted that within the treated area, water beads on the surface and runs down the stone façade, whereas outside the treated area water immediately penetrates the stone surface. Furthermore, the treatment does not appear to have accelerated weathering of adjacent untreated stone as evidenced by the consistency of the decay patterns. This raises the question of whether or not the treatment is making any difference at all to the durability of the treated stone as both the treated and untreated stone appears to be weath-

ering at a similar rate based on observed decay patterns. However, there may be noticeable differences in the condition of the subsurface of both treated and untreated stone, which could only be confirmed with further in situ investigations and possible sampling. As discussed in the introduction, when used incorrectly, hydrophobic treatments can accelerate physical weathering of stone due to changes in the mechanical properties of the stone and/or accumulation of salts behind the treated surface [26]. Decay patterns are identified and defined according to the ICOMOS-ISCS Illustrated glossary on stone deterioration patterns (2008). There are several prominent decay patterns present at Arbroath Abbey, as illustrated in Figure 5. Alveolisation is probably the most common decay pattern and is defined as the formation of cavities (alveoles) on the stone surface, which have variable shapes and sizes and may be connected [21]. At Arbroath, alveolisation is likely linked to the abundance of sea salts in the local atmosphere (Figure 5A) and potentially also the presence of carbonate in the stone (Section 4.3). Associated with alveolisation are salt deposits and efflorescence (Figure 5B). Detachment patterns are also common, primarily blistering (detachment of the outer stone layer leading to raised, air-filled hemispherical elevations) and delamination (detachment process affecting the laminated and/or bedded stones) [21] (Figure 5C,D). At Arbroath, delamination is associated with the weathering and detachment of stone layers along bedding planes. In these instances, the stones have been placed with bedding orientated parallel to the load of the building (face-bedded) (Figure 5D). Finally, the disintegration of the stone via sanding and differential erosion is common (Figure 5E,F). In this case, differential erosion occurs where the stones weather much faster than the surrounding mortar material. Delamination and blistering are the most common decay patterns on the studied façade, including the treated test area. Decay patterns are consistent across the treated and untreated areas of the façade.

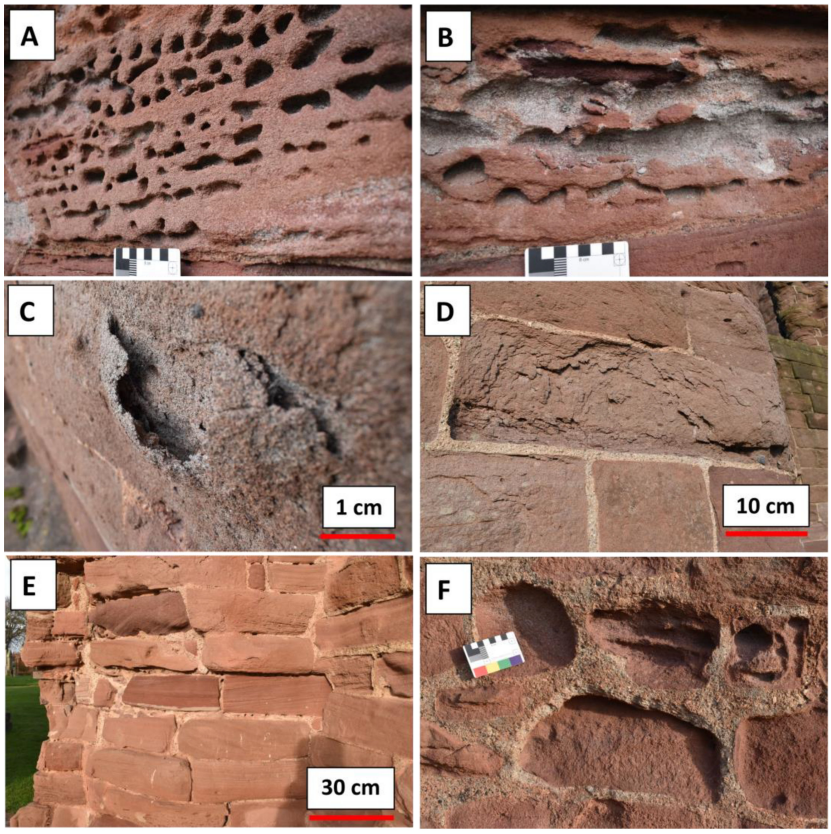

Figure 5. Prominent decay patterns identified at Arbroath Abbey. (**A**) = alveolisation; (**B**) = efflorescence and salt deposits; (**C**) = blistering*; (**D**) = lamination* (detachment of stone parallel to bedding) (* Prominent patterns on studied façade, including treated test area); (**E**) = sanding; (**F**) = differential weathering.

4.2. Moisture Mapping

A moisture analysis using a microwave moisture meter was carried out both when the façade was relatively dry and relatively wet. Figure 6 shows the entire façade in a fairly dry state, including the treated area highlighted in the red box. As seen from the moisture map, there are relative differences in the moisture content across the façade. The lower stones of the façade appear to be relatively wetter, perhaps indicating a degree of rising dampness. This possible rising dampness affects the treated area too (Figure 6). The efficacy of the water repellent was tested by wetting and then reanalysing part of the treated area (Figure 6). Only a small part of the treated area was studied in this way in order to avoid the possibility that some of the applied water would evaporate in the time between wetting and measurement. Figure 6 shows the relatively dry and wet state of the treated and adjacent area. Focusing on the area highlighted by the red box, there is a definite boundary where the subsurface of the stone is drier, suggesting less moisture ingress upon wetting. This result shows that the hydrophobic coating has retained a degree of water repellence some 40 years after its initial application.

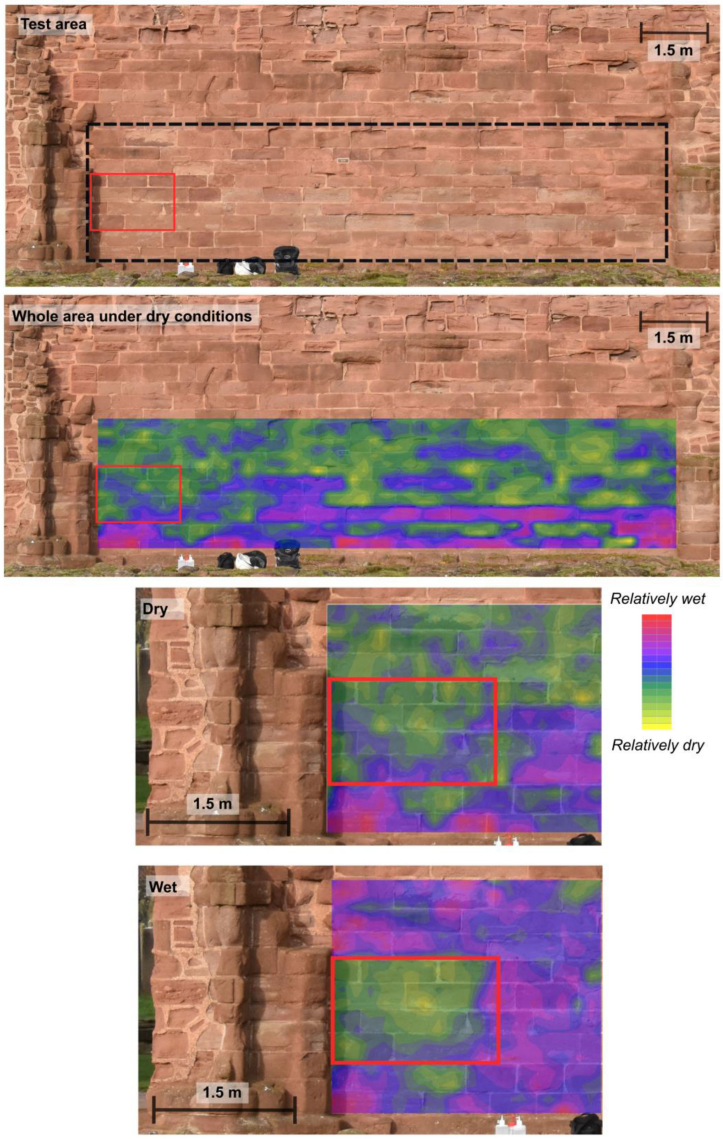

Figure 6. The upper half of the figure shows the relative dry state of the studied façade prior to any wetting. The lower half of the figure shows the treated area (outlined by the red box) before and after wetting of the façade. Yellow/green = relatively dry; pink/purple = relatively wet. Data represented in figure were acquired using an 11 cm probe head.

4.3. Mineralogy and Petrology

Overall, both sandstones (A-C and A-L) have a similar bulk mineralogy, as seen from the XRD results (Figure 7). The main difference is the presence of both orthoclase and albite in A-C, whereas A-L contains only orthoclase feldspar. Any differences between the interior and the crust of each sandstone are very small, although it does appear that the crust of both samples contains relatively more clay (as seen from the higher, well-defined clay peaks in the bulk analysis; Figure 7). The primary differences between sandstones A-C and A-L are the occurrence of smectite in A-C (Figure 7). We note that due to the small amount of smectite present, evidenced by the very small peaks, it is difficult to definitively identify the exact type of dioctahedral smectite present. The type of expansive clay can be narrowed down to montmorillonite, nontronite, or vermiculite, however.

Although present in the interior sandstone sample of A-C, smectite was consistently absent in the crust (outermost 5 mm of the stone). The clay mineralogy of the crust is dominated by kaolinite. This spatial difference in clay mineralogy implies that the in situ weathering of the building stone has altered the clay mineralogy at the stone surface over time, creating a clay-mineral profile through the stone. Smectite to kaolinite is a known weathering pathway in sediments and sandstones, primarily driven by the weathering of feldspars [27]. Previous research has identified weathering profiles in building stone through the analysis of total feldspar content and cation exchange capacities (CEC) [28,29]. Schäfer and Steiger (2002) attribute a lower CEC close to the surface to a reduction in the mineral surface area associated with clay dissolution. The clay mineralogy of the interior and crust samples of A-L are similar, which both show the presence of mainly kaolinite. Salts extracted from weathered sandstone near the treated site are halite and gypsum; these are typical coastal salts, which are not considered as aggressive as other salts (e.g.,: mirabilite, epsomite, hexahydrite, etc.) with regards to stone decay, but nonetheless will weather stone over time.

The petrography of the sandstones was characterised using optical microscopy and Backscattered Electron (BSE) and Secondary Electron (SE) imaging using SEM. The mineralogy was characterised further using Energy Dispersive X-ray (EDX) mapping. EDS shows that the composition of the feldspar grains varies, with A-L containing mostly orthoclase while A-C contains both orthoclase and albite. EDX mapping also shows the composition of material within the pore network. A-L pores are mostly filled with an Al-rich (clay) matrix while A-C pores are mostly empty or filled with carbonate cements. Optical and binocular microscopy shows the relative key differences in grain size, open porosity, and colour (Figure 8).

BSE and SEM analysis was carried out on thin sections and sandstone chips that were representative of the interiors of both stones (Figure 9A–H). The average grain size of A-C is 0.11 mm. Grain shape is subrounded where grain boundaries show long and concavo-convex contacts (Figure 9D). The matrix is sparse, although calcite is present both in the matrix and as a cementing material (Figure 9D). There is a higher proportion of lithic grains relative to A-L, and they have weathered extensively, leading to the formation of clay minerals with smectitic morphology (Figure 9A,B). The presence of lithic fragments weathering to smectite in this case is unsurprising given the amount of andesitic debris found locally, which has been recycled into many sandstone types in the area. Clay minerals exist as clasts or very thin grain coatings. The sandstone is poorly sorted and classified as a lithic arkose after Folk, 1974 [30].

The average grain size of A-L is 0.15 mm. Grain shape is angular to sub-rounded, and grain boundaries show point and long contacts (Figure 9G). The matrix and cements consist primarily of clay minerals, which are mostly kaolinite (Figure 9E). The degree of weathering is greater in A-L relative to A-C, as shown by the extent of mineral alteration and open pore space. Feldspars weather mostly to kaolinite (Figure 9H). An analysis of A-L sandstone chips also shows textures that appear to have preserved clay mineral transformation of a more smectite-like clay to kaolinite (Figure 9E), an observation consistent with the idea that smectite to kaolinite is a common clay mineral transformation for the studied Arbroath

stones. The greater extent of weathering in A-L relative to A-C may explain the absence of smectite, which has mostly weathered to kaolinite, as well as to illite-smectite and illite. Clay minerals are usually found in the matrix, cements, or coating grains. A-L is poorly sorted and classified as a lithic arkose after Folk, 1974 [30]. The petrography of A-L and A-C is summarised in Table 3.

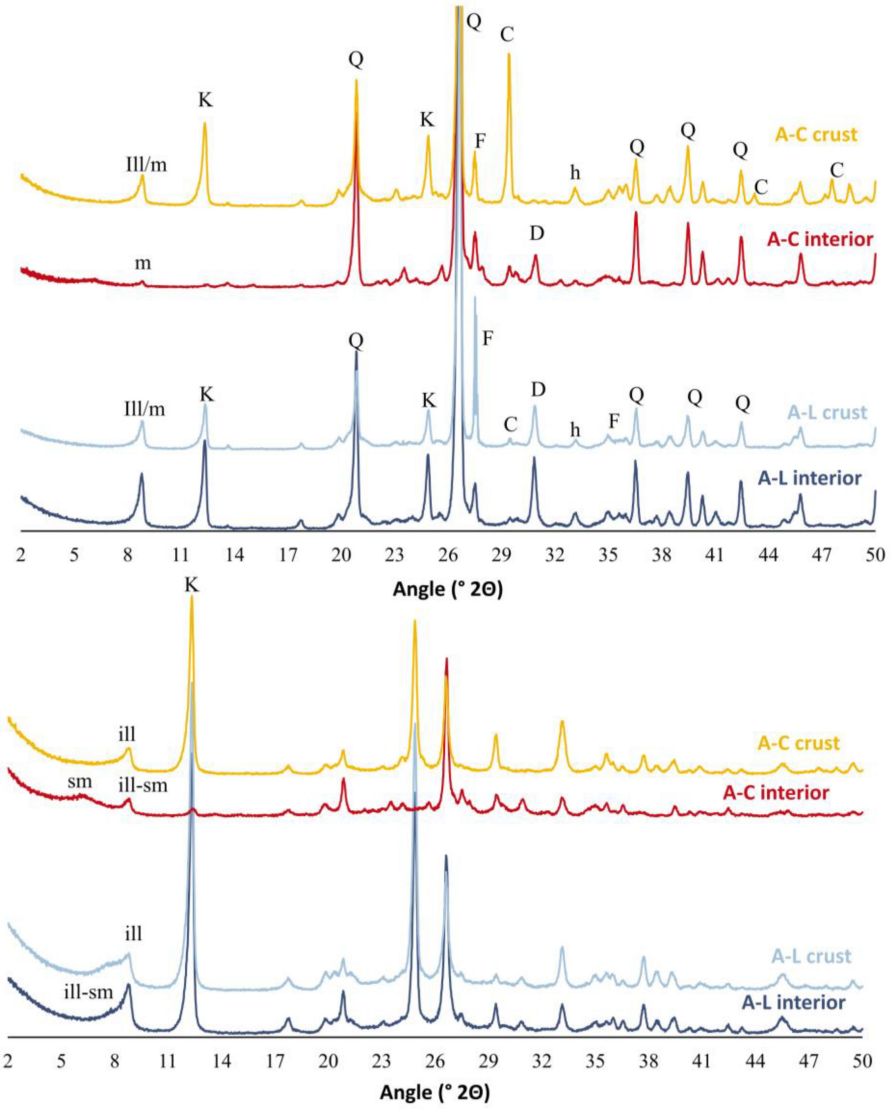

A-L

Mineral (%)	Interior	Crust
Quartz	66.9	35.0
Orthoclase	9.6	12.4
Muscovite	9.0	24.7
Kaolinite	7.6	18.8
Calcite	0.6	5.6
Dolomite	4.5	2.6
Hematite	1.8	0.9

A-C

Mineral (%)	Interior	Crust
Quartz	46.0	45.7
Orthoclase	14.0	7.3
Albite	12.0	19.1
Muscovite	19.0	5.0
Kaolinite	4.0	12.4
Calcite	2.0	8.3
Dolomite	2.0	-
Hematite	1.0	2.2

Figure 7. Bulk mineralogy (top two pairs of diffractograms) and clay mineralogy (bottom two pairs of diffractograms) of interior and crust samples for both A-C and A-L. Labelled peaks are as follows: Q = quartz; F = feldspars; K = kaolinite; ill = illite; m = muscovite; C = calcite; h = hematite; sm = smectite; ill-sm = interstratified illite-smectite. Semi-quantitative mineral contents (%) of the bulk mineralogy of both interior and crust samples are shown in tables.

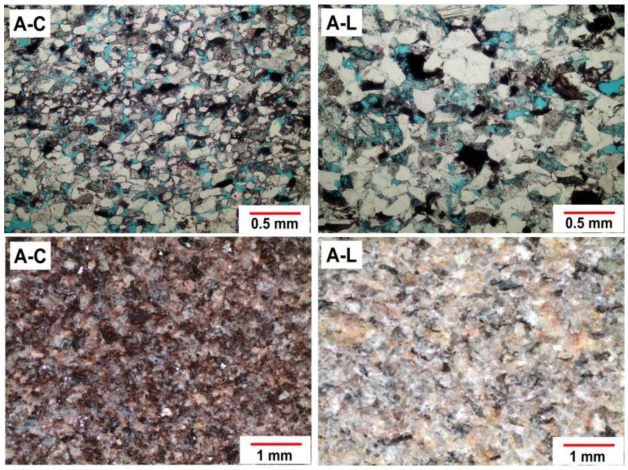

Figure 8. Optical (**top**) and binocular (**bottom**) images of studied sandstones A-C and A-L showing key differences in grain size and colour.

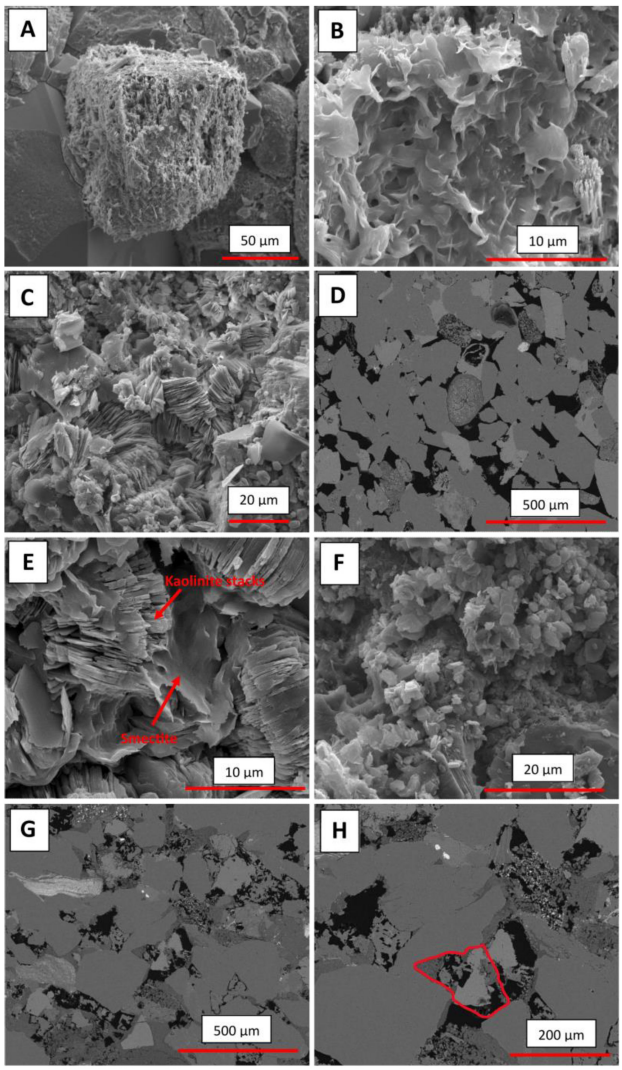

Figure 9. SEM images of analysed A-C (**A**–**D**) and A-L (**E**–**H**) sandstone samples. (**A**) Weathered lithic grain leading to formation of a clay mineral with smectitic morphology; (**B**) Smectitic morphology of clay found on grain surface of (**A**); (**C**) Preservation of a clay mineral transformation, likely smectite to kaolinite; (**D**) Thin section of A-C showing mostly quartz (relatively dark-coloured grains), feldspars

(relatively light-coloured grains), weathered lithics (e.g., centre), and empty pore space (black). (**E**,**F**) Diagenetic kaolinite representing most common clay mineral found in A-L. (**E**) Change in morphology of clay from 'leafy' smectite morphology to a more typical kaolinite stack morphology. (**G**) BSE image highlighting distribution of clay minerals, which is mainly coating grains, lining pores, and partially infilling pores and pore throats. (**H**) Higher magnification BSE image of (**G**), showing diagenetic kaolinite replacing detrital feldspars (original grain outlined in red).

Table 3. Summary of the mineralogy and petrography of A-C and A-L based on XRD and SEM results.

	A-C		**A-L**	
	Interior	**Exterior**	**Interior**	**Exterior**
Bulk mineralogy	Quartz; albite; orthoclase; calcite; dolomite	Quartz; albite; orthoclase; calcite; hematite; kaolinite; illite	Quartz; albite; orthoclase; dolomite; mica; kaolinite; illite; hematite	Quartz; albite; orthoclase; dolomite; mica; kaolinite; illite; hematite
Clay mineralogy	kaolinite; smectite (expansive); illite-smectite (non-expansive)	kaolinite; illite	illite-smectite (non-expansive); kaolinite	kaolinite; illite
Clay distribution	Weathered lithics; weathered feldspars; lining pores	Infilling pores; coating grains	Matrix; grain coatings; weathered feldspars	Matrix; infilling pores; coating grains
Average grain size (mm)	0.11		0.15	
Sandstone classification [1]	Lithic arkose		Lithic arkose	

[1] Based on Folk (1974) classification scheme [27].

4.4. Open Porosity

The open porosity varies considerably, from 11.5–21.8% and 13.9–23.2% for A-C and A-L, respectively (Table 4). The average porosity for A-C is 14.7% and for A-L is higher at 19.3%. As seen from Table 4, there is a relationship between porosity and bulk density, with higher porosity samples having a lower bulk density. This lower density reflects the relative abundance of pore space.

Table 4. Average open porosity, bulk density, and capillary absorption coefficient before (C_U) and after (C_T) application of the hydrophobic treatment. Initially the samples were measured parallel (–) and perpendicular (+) to bedding to understand the degree of sandstone anisotropy with regards to capillary absorption. After treatment, the samples were measured parallel to bedding only. This direction was selected as it reflects the orientation of bedding–water interactions in most buildings. Consequently, transport of water and efficiency of any treatments are best evaluated in this direction.

	Porosity, P_o (%)	**Bulk Density (g/cm^3)**	**Capillary Absorption Coefficient, C_U [kg/(m^2·h$^{0.5}$]**		**Capillary Absorption Coefficient, C_T [kg/(m^2·h$^{0.5}$]**
			–	+	–
A-C	14.7 ± 4.16 [1] (21)	2.39 ± 0.12 (21)	0.95 ± 1.69 [1] (6)	0.17 ± 0.23 [1] (6)	0.37 ± 0.22 (6)
			–	+	–
A-L	19.3 ± 3.37 (21)	2.24 ± 0.10 (21)	1.98 ± 0.28 (6)	1.49 ± 0.41 (6)	0.24 ± 0.11 (6)

[1] High standard deviations, of A-C samples in particular, reflect the heterogeneity of sandstone samples. Numbers in parentheses indicate the number of samples analysed and used to calculate an average value.

4.5. Capillary Absorption

There was considerable variation in the capillary absorption rates both between and within sandstones A-C and A-L. This variation is likely linked to porosity differences between individual samples of the same block. Overall, A-L has a faster average rate of capillary absorption, and so higher capillary absorption coefficient (Table 4). Both samples show a degree of anisotropy–variation in capillary absorption rates when measured in two different directions. Both sandstones show a faster rate of capillary absorption when measured parallel to bedding, where water can be absorbed along bedding planes. The anisotropic behaviour of bedded sandstones related to capillary absorption is well documented in the literature [31–35]. The degree of anisotropy is calculated using the minimum value divided by the maximum value for a given measured property. Therefore, values close to 1 indicate a homogenous stone, where there is little to no variation, and values close to 0 indicate a heterogenous stone, where there is considerable variation for a given measured property. The anisotropy is stronger in A-C at 0.18 in comparison to A-L at 0.75.

Finally, the capillary absorption of A-C and A-L was measured after the samples had received the hydrophobic treatment. The capillary absorption after treatment was only measured in the direction parallel to the bedding, as this is reflective of the direction of the moisture ingress onsite at the Abbey. The overall aim of the treatment is to reduce the rate of capillary absorption of the treated sample to as low as possible. The efficiency of the treatment in reducing the capillary absorption was variable and less effective for A-C (average reduction of 61%) relative to A-L (average reduction of 88%) (Table 4). The less effectively reduced capillary absorption of A-C implies a lower penetration depth of the hydrophobic cream. As the application process for the treatment was identical for all samples, the lower penetration depth associated with A-C is ultimately driven by the petrophysical properties of the stone including lower capillary absorption (prior to treatment) and lower porosity, relative to A-L. This trend was similar when comparing sandstone samples from the same block, where the treatment was less effective in reducing the capillary absorption of samples which had a lower porosity and lower capillary absorption rate prior to treatment (Figure 10). The variability in physical properties of individual stones and their response to the hydrophobic treatment highlight some potential issues with regards to large scale treatment of the stone at Arbroath Abbey. Despite the uniform application of the treatment, variations in physical properties between and within individual blocks may lead to differences in the efficiency of a hydrophobic treatment. The potential variation in the treatment efficiency may make certain stones more susceptible to weathering and exacerbate differential weathering.

4.6. Vapour Diffusion Resistance

The assessment of water vapour diffusion resistance is considered essential for understanding the compatibility of a given stone and hydrophobic treatment [20,36]. The water vapour diffusion resistance factor was calculated before and after treatment using the same samples. The resistance factor and associated porosity of each sample is shown in Table 5. An increase in the diffusion resistance up to ~20% is considered acceptable according to Snethlage (2011) [17]. As seen from Table 5, A-C3 is the only sample that surpasses a 20% increase in resistance after treatment. This compares to another sample of A-C, A-C1, where resistance increases by only ~4%, again highlighting the implications of variations in physical properties associated with heterogenous stone for the efficiency of a hydrophobic treatment. Similarly, A-L shows a ~4–18% increase in resistance.

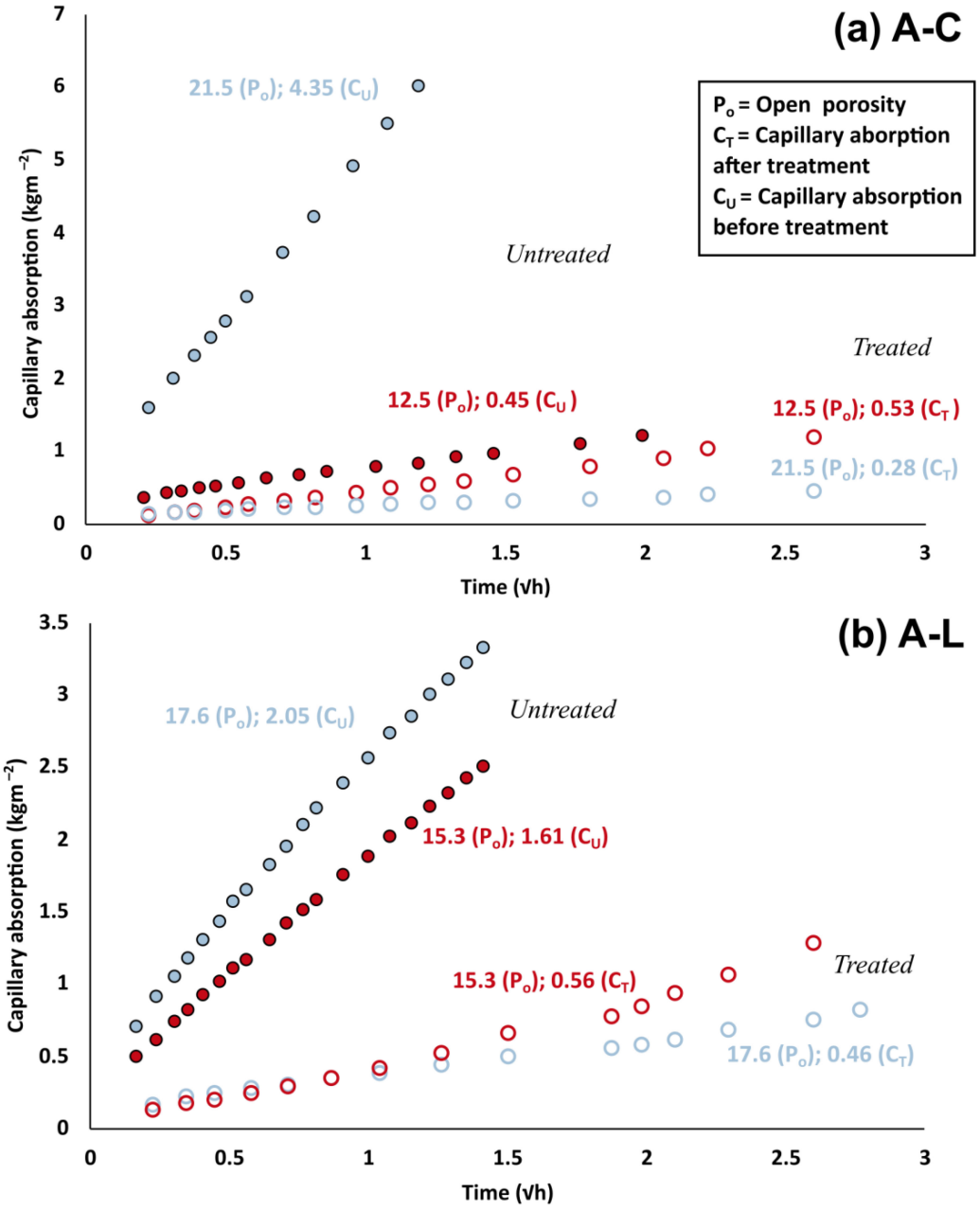

Figure 10. Capillary absorption of (**a**) A–C (high and low porosity examples) before and after application of hydrophobic treatment and (**b**) A–L (high and low porosity examples) before and after treatment. Samples before application of hydrophobic treatment are represented by filled circles, and samples after hydrophobic treatment are represented by open circles.

Table 5. Vapour diffusion resistance factor before and after treatment with hydrophobic coating.

	Resistance Factor, μ	Resistance Factor, μ_t	Change in Resistance, %	Porosity, P_o (%)
A-C1	42.3	44.1	4.3	11.5
A-C2	50.1	58.3	16.4	11.7
A-C3	32.6	41.1	26.1	10.6
A-L1	27.1	28.1	3.7	22.8
A-L2	23.7	26.8	13.1	22.6
A-L3	31.2	36.7	17.6	17.4

4.7. Durability

In laboratory studies, decay is quantified as the change in dry mass at the end of a salt weathering experiment [37]. Figure 11 shows the typical relative changes in the mass of a sample throughout the experiment. The mass during the experiment (7th cycle) and at the end prior to salt extraction (20th cycle) is higher than the original mass. This difference represents the presence of crystallised salts within the sample. After salt extraction at the end of the experiment the mass is (usually) lower than the original weight if weathering has occurred.

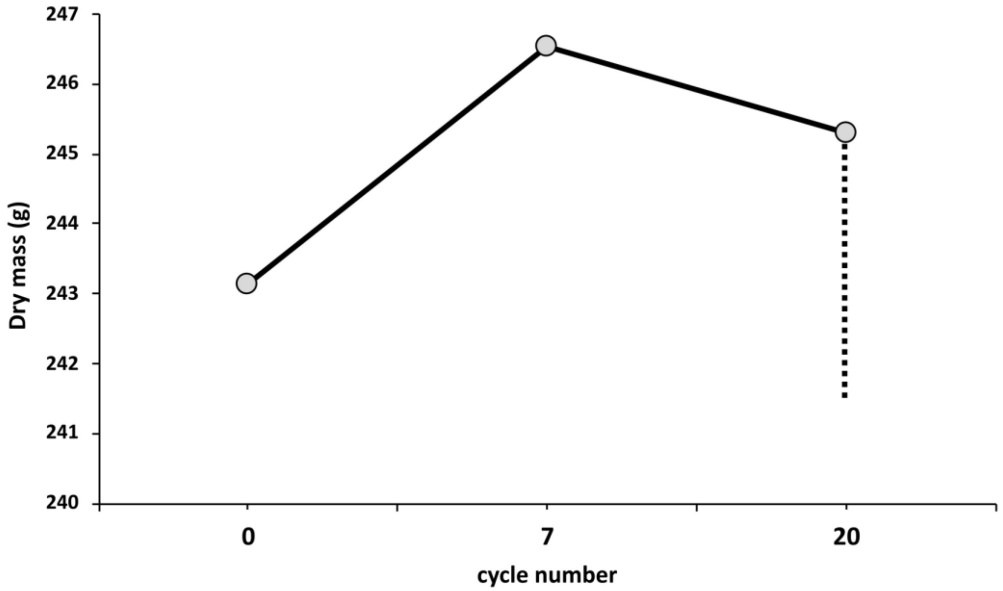

Figure 11. Example of A-L sample illustrating the relative changes in mass throughout the salt weathering experiment. The mass during the experiment (7th, 20th cycles) is higher than the original mass due to the presence of salts. The final mass obtained after cycle 20 is after removal of salts.

Overall, untreated samples of both A-C and A-L were more susceptible to decay than treated ones, as reflected by the higher values of the percentage decay (Figure 12). The values for the decay of the treated samples are all negative, suggesting the presence of salts within pores after salt extraction (Table 6). However, sandstones commonly contain some salts even after salt extraction. Overall, it is likely that the treated samples also experienced less decay relative to the untreated samples due to the hydrophobic treatment limiting the moisture ingress. From a visual assessment, the decay of both treated and untreated samples is very minor and unnoticeable, although decay usually manifests as granular disintegration. For most individual samples, V_p is less after the experiments, reflecting an increase in the pore space associated with weathering (Table 6). In some individual cases, the V_p is higher after the experiment, which may reflect the presence of salts within samples. Generally, there is not much difference in the behaviour of V_p between treated and untreated samples.

A-L was slightly more susceptible to decay, expressed as weight loss, in comparison to A-C, as represented by the higher values of decay associated with A-L (Table 6). The higher susceptibility of A-L to weathering may be linked to the original porosity of the stone, which is, on average, slightly higher than that of A-C (Figure 12). The porosity of the untreated samples was slightly higher after weathering reflecting more open pore space due to decay. The porosity of treated sandstone samples was slightly lower after weathering, implying the presence of salts and/or that little weathering has taken place.

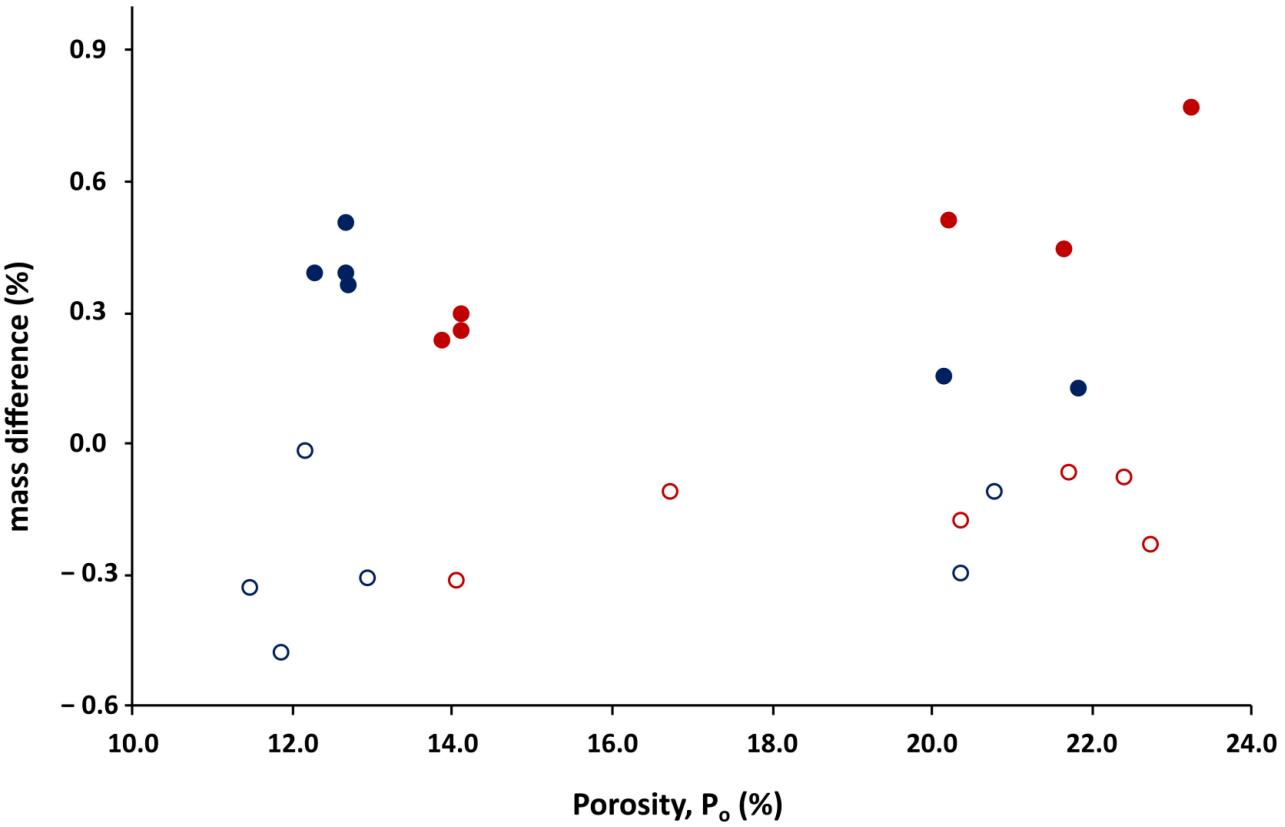

Figure 12. The relationship between P_o (%) and material loss (decay) of A-C (blue circles) and A-L (red circles). Treated samples were less prone to decay overall while untreated samples experienced relatively higher amounts of decay. Note negative values imply presence of salts in addition to less decay. Open circles are treated samples after weathering and solid circles are untreated samples after weathering.

Table 6. Summary of salt weathering results: Average values of six samples for: open porosity before and after weathering (P% and $P_{o\text{-}w}$ respectively); p-wave velocities before and after weathering (Vp and Vp_w respectively); capillary absorption coefficient before and after weathering (C and C_w respectively); and decay as a result of weathering expressed as percentage weight loss (d%). U = prior to application of hydrophobic treatment (untreated); T = after application of hydrophobic treatment (treated). Numbers in parentheses indicate the number of samples analysed and used to calculate an average value.

	A-C_U	**A-C_T**	**A-L_U**	**A-L_T**
P_o (%)	15.4 ± 4.38	14.9 ± 4.40	17.9 ± 4.31	19.7 ± 3.52
$P_{o\text{-}w}$ (%)	16.0 ± 4.22	14.0 ±4.55	18.5 ±4.96	19.3 ± 3.62
V_p (m/s)	3219.6 ± 433.8	3546.0 ± 399.6	3206.1 ±279.3	3284.6 ± 162.8
$V_{p\text{-}w}$ (m/s)	3114.4 ± 215.7	3359.0 ± 287.2	3117.8 ± 104.5	3133.4 ± 160.2
C [kg/(m^2·h$^{0.5}$)]	1.65 ± 1.86	0.34 ± 0.22	1.33 ± 0.55	0.27 ± 0.07
C_w [kg/(m^2·h$^{0.5}$)]	2.30 ± 2.05	0.42 ± 0.29	1.57 ± 0.55	0.34 ± 0.13
d (%)	0.32 ± 0.15	−0.25 ± 0.17	0.42 ± 0.20	−0.16 ± 0.10

On average and for most of the individual samples, the capillary absorption coefficient is higher after salt weathering, suggesting an increase in porosity, leading to an increase in capillary absorption (Table 6). A-L samples (both treated and untreated) experienced a higher percentage increase in capillary absorption on average compared to A-C. Again, this probably relates back to the slightly higher open porosity of A-L. There is little difference in the capillary absorption increase after weathering when comparing treated and untreated samples.

5. Final Discussion and Conclusions

The objectives of the study were twofold: (1) to perform a moisture mapping of an area at Arbroath Abbey previously treated with a silane-based hydrophobic product for the first time since its initial application over 40 years ago; and (2) to evaluate the compatibility of a currently available silane-based hydrophobic product with weathered sandstone from the Abbey. In this study we utilized both field-based moisture analysis and lab-based stone characterisation tests to better understand the long-term behaviour and compatibility of hydrophobic treatments in protecting vulnerable sandstone, by reducing the rate of stone decay. Having the ability to conduct field-based analysis on an area of sandstone masonry treated over 40 years and obtain a high volume of untreated stone of the same type for lab-based characterisation is a rare opportunity. The moisture analyses, along with our initial inspection at the Abbey in 2017, has shown that the silane-based Brethane treatment is still providing the sandstone with a degree of water repellency some 40 years after its application in 1976. Moreover, moisture analyses have highlighted external factors that may be influencing the efficiency of the treatment by providing insight into the relative differences of moisture content across the entire façade of interest. These external factors include a potential rising dampness issue, as evidenced by a relative increase in the moisture content across the lower part of the façade. Price (1981) noted that Brethane, among other silane-based treatments, was not suitable for stones that contained an abundance of sodium chloride ('sea salt') or at sites affected by rising dampness problems [4]. Interestingly, both sea-derived salts and rising dampness (see above) are present at Arbroath Abbey, yet the Brethane treatment appears to be performing well. The lab-based accelerated salt weathering experiments have shown that the application of the silane-based treatment reduces the rate of stone decay experienced by the sample.

However, the differences in intrinsic stone properties between lab-analysed stone samples A-C and A-L, mainly porosity and capillary absorption, evidently affect the performance of the hydrophobic treatment. For example, due to the higher porosity and capillary absorption rates of A-L, the cream was able to penetrate deeper into the sample during the application, reducing the capillary absorption far more effectively than in the case of A-C. Furthermore, petrophysical properties and mineralogy vary within the individual stone types. For example, the open porosity of A-C varied between ~11 and 21%, and the vapour diffusion resistance factor of the same stone ranged from ~33 to 50. All of these differences between and within samples mean that despite an identical approach to the application of a hydrophobic cream, individual blocks of stone can respond very differently when such a treatment is applied on site. Varying responses to treatment could lead to differential weathering as a consequence of some parts of a façade being better protected than others. Differential weathering is a concern commonly mentioned in the literature regarding hydrophobic treatments, especially in the context of heterogenous stone types [38–42].

Together the field-based and lab-based investigations provide more information on the potential use of silane-based hydrophobic treatments in protecting vulnerable sandstone at Arbroath Abbey. Both parts of the study suggest that such treatments can be used successfully in protecting sandstone when applied correctly, by reducing rate of decay, and reducing moisture ingress over long periods of time. However, the heterogeneity of sandstone may mean that some individual stones are less compatible with the hydrophobic treatment tested than others. Further field-based analyses of the treated area (including methods such as XRF and in situ vp) are required in order to determine the state of conservation of the treated area more accurately. Sampling the treated area would also provide invaluable insight into the properties of the treated surface and subsurface and in particular the relationship between salts and the hydrophobic layer. Finally, an important caveat to consider in this study is that despite the similarities between the silane-based treatments assessed both in situ and in the lab, they are different products, which to an extent limits our direct comparison of in situ and lab-based analyses.

More broadly, the mineralogical results obtained as part of this study have significant implications for sampling at heritage sites. As stone decay studies often deal with valuable materials, sampling can be heavily restricted. For this reason, small samples of crust or highly weathered samples are often used for XRD and SEM characterisations. However, as demonstrated by our research, such deteriorated material may not be reflective of the overall mineralogy of the stone, especially in the case of less stable expansive clays, which may have weathered and changed in character at the surface that are still present in the interior of the stone. This sampling issue may mean that smectite is under-represented in many previous stone characterisation studies.

Employing a single hydrophobic product that is equally compatible with every stone at a given site is unrealistic, especially in cases such as Arbroath Abbey where the constituent sandstone is heterogenous. In the case of the Abbey stones studied, the efficiency of treatment varies both between and within the individual stone types. Despite some of the obvious drawbacks of using hydrophobic treatments in conjunction with heterogenous stone types, such options may still need to be considered more seriously in Scotland and indeed elsewhere as a result of climate change. Increases in precipitation and the intensity of precipitation may enhance moisture ingress and lead to prolonged stone wetness. It is therefore imperative to continue to explore any options that potentially limit the amount of moisture penetrating the stone, thus limiting stone decay. This may be especially important for build sites of extreme cultural value and significance that are very close to ruin and where suitable alternative conservation methods have not been identified.

Author Contributions: Conceptualization, M.d.J.; methodology, M.d.J., D.B., C.G. and M.Y; software, M.d.J. and M.Y.; formal analysis, M.d.J., D.B., C.G. and M.Y.; investigation, M.d.J., D.B., C.G. and M.Y.; resources, M.d.J., M.Y., M.L. and D.B.; data curation, M.d.J.; writing—original draft preparation, M.d.J.; writing—review and editing, M.L. and D.B.; visualization, M.d.J.; supervision, M.L.; project administration, M.d.J.; funding acquisition, M.d.J., M.L. and M.Y. All authors have read and agreed to the published version of the manuscript.

Funding: This research was funded by the University of Glasgow and Historic Environment Scotland as part of a fully-funded Ph.D. project (HES project number: 301140). The British Geological Survey (BGS) supported preparation and revision of the manuscript.

Data Availability Statement: The data is available and those interested are encouraged to contact the lead author (M.d.J.).

Acknowledgments: M.d.J. would like to thank all of the authors for their contributions to the current paper and also their constant support throughout the entire Ph.D. project.

Conflicts of Interest: The authors declare no conflict of interest.

References

1. Young, M.; Murray, M.; Cordiner, P. *Chemical Consolidants and Water Repellents for Sandstones in Scotland*; Historic Environment Scotland: Edinburgh, UK, 2003.
2. Öztürk, I. Alkoxysilanes Consolidation of Stone and Earthen Building Materials. Master's Thesis, University of Pennsylvania, Philadelphia, PA, USA, 1992.
3. Odgers, D. Progress with Stone Consolidants; Historic England, The Institute of Historic Building Conservation (IHBC), UK. 2018, pp. 20–22. Available online: https://historicengland.org.uk/content/docs/research/ctx154-odgers-stone-consolidantspdf/ (accessed on 1 May 2023).
4. Price, C.A. *Brethane Stone Preservative: Current Paper CP1/81, 1-9*; Building Research Establishment: Watford, UK, 1981.
5. Garcia Pascua, N.; Sánchez De Rojas, M.I.; Frias, M. The important role of the color measurement in restoration works: Use of consolidants and water-repellents in sandstone. In Proceedings of the 8th Eighth International Congress on Deterioration and Conservation of Stone Proceedings, Berlin, Germany, 30 September–4 October 1996; pp. 1351–1361.
6. Cnudde, V.; Jacobs, P.J.S. Monitoring of weathering and conservation of building materials through non-destructive X-ray computed microtomography. *Environ. Geol.* **2004**, *46*, 477–485. [CrossRef]
7. Jiménez González, I.; Scherer, G.W. Effect of swelling inhibitors on the swelling and stress relaxation of clay bearing stones. *Environ. Geol.* **2004**, *46*, 364–377. [CrossRef]
8. De Ferri, L.; Lottici, P.P.; Lorenzi, A.; Montenero, A.; Salvioli-Mariani, E. Study of silica nanoparticles–polysiloxane hydrophobic treatments for stone-based monument protection. *J. Cult. Herit.* **2011**, *12*, 356–363. [CrossRef]

9. Pinna, D.; Salvadori, B.; Galeotti, M. Monitoring the performance of innovative and traditional biocides mixed with consolidants and water-repellents for the prevention of biological growth on stone. *Sci. Total Environ.* **2012**, *423*, 132–141. [CrossRef] [PubMed]
10. Akoğlu, K.G.; Caner-Saltık, E.N. Hydric dilation of Mount Nemrut sandstones and its control by surfactants. *J. Cult. Herit.* **2015**, *16*, 276–283. [CrossRef]
11. Wen, Y.; Qing, H.; Shu, H.; Liu, Q. Evaluating the Protective Effects of Calcium Carbonate Coating on Sandstone Cultural Heritage. *Coatings* **2021**, *11*, 1534. [CrossRef]
12. Elert, K.; Rodriguez-Navarro, C. Degradation and conservation of clay-containing stone: A review. *Constr. Build. Mater.* **2022**, *330*, 127226. [CrossRef]
13. Charola, A.E. Water Repellents and Other" Protective" Treatments: A Critical Review/Hydrophobieren und andere" schützende" Maßnahmen: Ein kritischer Überblick. *Restor. Build. Monum.* **2003**, *9*, 3–22. [CrossRef]
14. Moropoulou, A.; Kouloumbi, N.; Haralampopoulos, G.; Konstanti, A.; Michailidis, P. Criteria and methodology for the evaluation of conservation interventions on treated porous stone susceptible to salt decay. *Prog. Org. Coat.* **2003**, *48*, 259–270. [CrossRef]
15. Jia, M.; Liang, J.; He, L.; Zhao, X.; Simon, S. Hydrophobic and hydrophilic SiO_2-based hybrids in the protection of sandstone for anti-salt damage. *J. Cult. Herit.* **2019**, *40*, 80–91. [CrossRef]
16. Ershad-Langroudi, A.; Fadaei, H.; Ahmadi, K. Application of polymer coatings and nanoparticles in consolidation and hydrophobic treatment of stone monuments. *Iran. Polym. J.* **2019**, *28*, 1–19. [CrossRef]
17. Gherardi, F. Current and Future Trends in Protective Treatments for Stone Heritage. In *Conserving Stone Heritage*; Springer: Cham, Switzerland, 2022; pp. 137–176.
18. Kennedy, C.J. The role of heritage science in conservation philosophy and practice. *Hist. Environ. Policy Pract.* **2015**, *6*, 214–228. [CrossRef]
19. *WTA Merkblatt AG 3.17*; Hydrophobierende Imprägnierung von mineralischen Baustoffen. WTA Publications: Stuttgart, Germany, 2010.
20. Snethlage, R. Stone Conservation. In *Stone in Architecture*; Springer: Berlin/Heidelberg, Germany, 2011; pp. 516–518.
21. Vergès-Belmin, V. (Ed.) *Illustrated Glossary on Stone Deterioration Patterns*; *Monuments and Sites XV*; ICOMOS: Paris, France, 2008.
22. *BS EN 1936:2006*; Natural Stone Test Methods—Determination of Real Density and Apparent Density, and of Total and Open Porosity. BSI: London, UK, 2006.
23. *BS EN 12572:2016*; Hygrothermal performance of building materials and products—Determination of water vapour transmission properties—Cup method. BSI: London, UK, 2016.
24. *BS EN ISO 15148:2002*; Hygrothermal performance of building materials and products—Determination of water absorption coefficient by partial immersion. BSI: London, UK, 2002.
25. Benavente, D.; del Cura, M.G.; Bernabéu, A.; Ordóñez, S. Quantification of salt weathering in porous stones using an experimental continuous partial immersion method. *Eng. Geol.* **2001**, *59*, 313–325. [CrossRef]
26. Charola, A.E.; Bläuer, C. Salts in masonry: An overview of the problem. *Restor. Build. Monum.* **2015**, *21*, 119–135. [CrossRef]
27. McKinley, J.M.; Worden, R.H.; Ruffell, A.H. Smectite in sandstones: A review of the controls on occurrence and behaviour during diagenesis, clay mineral cements in sandstone. *Int. Assoc. Sedimentol. Spec. Publ.* **2003**, *34*, 109–128.
28. Mausfeld, S.A.; Grassegger, G. Abbauprozesse an Feldspaten und Tonmineralen unter den Bedingungen der Bauwerksverwitterung. *Z. Dt. Geol. Ges.* **1992**, *143*, 23–39.
29. Schäfer, M.; Steiger, M. A rapid method for the determination of cation exchange capacities of sandstone: Preliminary data. In *Natural Stone, Weathering Phenomena, Conservation Strategies and Case Studies*; Siegesmund, S., Weiss, T., Vollbrecht, A., Eds.; Geological Society, Special Publications: London, UK, 2002; Volume 205, pp. 431–439.
30. Folk, R.L. *Petrology of Sedimentary Rocks*; Hemphill Publishing Company: Austin, TX, USA, 1980.
31. Ruedrich, J.; Siegesmund, S. Salt and ice crystallisation in porous sandstones. *Environ. Geol.* **2007**, *52*, 225–249. [CrossRef]
32. Sebastián, E.; Cultrone, G.; Benavente, D.; Fernandez, L.L.; Elert, K.; RodriguezNavarro, C. Swelling damage in clay-rich sandstones used in the church of San Mateo in Tarifa (Spain). *J. Cult. Herit.* **2008**, *9*, 66–76. [CrossRef]
33. Benavente, D.; Cultrone, G.; Gómez-Heras, M. The combined influence of mineralogical, hygric and thermal properties on the durability of porous building stones. *Eur. J. Mineral.* **2008**, *20*, 673–685. [CrossRef]
34. Zhao, J.; Plagge, R. Characterization of hygrothermal properties of sandstones—Impact of anisotropy on their thermal and moisture behaviors. *Energy and Buildings* **2015**, *107*, 479–494. [CrossRef]
35. Fořt, J. Effect of Sandstone Anisotropy on its Heat and Moisture Transport Properties. *Mater. Sci.* **2015**, *21*, 455–459. [CrossRef]
36. Ludovico-Marques, M.; Chastre, C. Effect of consolidation treatments on mechanical behaviour of sandstone. *Constr. Build. Mater.* **2014**, *70*, 473–482. [CrossRef]
37. Siegesmund, S.; Dürrast, H. Physical and mechanical properties of rocks. In *Stone in Architecture*; Springer: Berlin/Heidelberg, Germany, 2011; pp. 97–225.
38. Charola, A.E. Water Repellents and Other "Protective" Treatments: A Critical Review. In Proceedings of the Hydrophobe III–3rd International Conference on Surface Technology with Water Repellent Agents, Hannover, Germany, 25–26 September 2001; pp. 3–20.
39. Angeli, M.; Bigas, J.P.; Benavente, D.; Menéndez, B.; Hébert, R.; David, C. Salt crystallization in pores: Quantification and estimation of damage. *Environ. Geol.* **2007**, *52*, 205–213. [CrossRef]

40. McKinley, J.M.; Warke, P.A. Controls on permeability: Implications for stone weathering. *Geol. Soc. Lond. Spec. Publ.* **2007**, *271*, 225–236. [CrossRef]
41. McAllister, D.; Warke, P.; McCabe, S.; Gomez-Heras, M. Evaporative moisture loss from heterogeneous stone: Material-environment interactions during drying. *Geomorphol.* **2016**, *273*, 308–322. [CrossRef]
42. Zoghlami, K.; López-Arce, P.; Zornoza-Indart, A. Differential stone decay of the Spanish tower façade in Bizerte, Tunisia. *J. Mater. Civ. Eng.* **2017**, *29*, 05016005. [CrossRef]